Journal of Applied Polymer Science

Stress–Thermooxidative Aging Behavior of Polyamide 6

Xiaowen Zhao, Xiaohe Li, Lin Ye, Guangxian Li
State Key Laboratory of Polymer Materials Engineering, Polymer Research Institute of Sichuan University, Chengdu 610065, China
Correspondence to: L. Ye (E-mail: yelinwh@126.com)

ABSTRACT: The long-term stress–thermooxidative aging behavior of polyamide 6 (PA6) was studied in terms of the creep behavior, mechanical properties, chemical structure, crystallization, and orientation behavior. During aging, a thermooxidation reaction occurred, which included molecular chain degradation and crosslinking, in PA6. Meanwhile, when the samples were subjected to stress, crystallization, orientation, and chain scission were induced. In the initial stages of aging, the stress-induced crystallization and orientation dominated; this resulted in an increase in the creep deformation, mechanical strength, crystallinity, and orientation factor. Molecular degradation and chain scission dominated in the subsequent aging process and resulted in a decrease of the mechanical strength, reduced viscosity, crystallinity, and orientation factor and an increase in the formation of oxide and peroxide products. The stress may have promoted the chain scission of PA6 during thermal aging and resulted in a decrease in the reduced viscosity and an increase in the carboxylic acid concentration. © 2012 Wiley Periodicals, Inc. J. Appl. Polym. Sci. 129: 1193–1201, 2013

KEYWORDS: aging; mechanical properties; polyamides

Received 14 September 2012; accepted 19 September 2012; published online 27 November 2012
DOI: 10.1002/app.38616

INTRODUCTION

Polyamide 6 (PA6) has been one of the most widely used engineering thermoplastics since I. G. Farbenindustrie commercially developed it in about 1940.[1] It has been largely applied in the forms of fibers and molded parts because of its excellent mechanical properties and high thermal resistance.

Polyamides (PAs) are sensitive to oxygen and continuously oxidize in ambient atmosphere; this results in the subsequent deterioration of its properties. Thus, phenomena such as gradually increasing yellowing and eventual embrittlement are clearly observable. The thermooxidation of PA occurs predominantly through the abstraction of a hydrogen atom on the methylene groups close to the nitrogen of the amide group (—CO—NH—CH_2—).[2~6] Considerable research has focused on the thermooxidative aging behavior of PA.[7–15] However, in the course of its use, the external mechanical stress can also cause molecular degradation and physical and chemical changes in the molecular structure, which affect the aging behavior, performance, and service lifetime of PA. Therefore, it is very important to simulate the aging behavior of PA under stress.

Until now, little information has been available for investigations of the stress-accelerated aging behavior of PA6, just the work of Jacobson et al.,[16] who studied the effect of the stress on the oxidation degradation of PA6 with the method of stress–chemiluminescence. On the basis of their results, they concluded that stresses up to 80% of load at yield did not change the rate of oxidation of the PA6 film.[16] The aging mechanism of PA6 under stress remains relatively unexplored.

In our previous work, we studied the long-term stress-accelerated aging behavior of PA6 by exposing it to UV irradiation, and in this study, we studied the long-term stress-accelerated aging behavior of PA6 at relatively high temperatures. The aging behavior and mechanism were investigated in terms of the creep behavior, mechanical properties, molecular structure, orientation, and crystallization behavior. On the basis of these results, we made an attempt to gain a better understanding of the influence of the stress and temperature on the thermooxidative degradation of PA 6.

EXPERIMENTAL

Materials

The PA6 used in this work was a commercial-grade granular product (YH800) without any additives (Yueyang Petrochemical Co., Ltd., Hunan, China); it had a relative viscosity of 2.85 ± 0.03 in formic acid. Samples of PA6 were prepared by injection molding into standard dumbbell and rectangular splints (length = 155 mm, thickness = 4.2 mm).

Applied Polymer SCIENCE

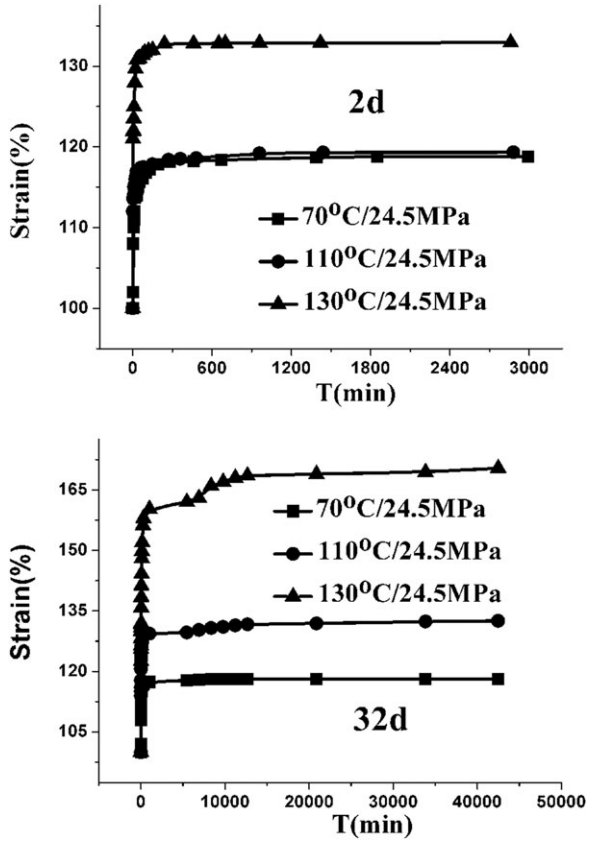

Figure 1. Strain of PA6 as a function of the aging time at different temperatures under 24.5 MPa (T = time).

Stress–Thermooxidative Aging of PA6

Standard dumbbell-shaped samples of nylon 6 were subjected to tensile stress at different temperatures on a self-made stretching apparatus. The samples were taken out at regular time intervals for mechanical and chemical characterization.

Measurement

Mechanical Properties. The tensile and bending performances of PA6 samples were measured with a 4302 material testing machine from Instron Co. (Norwood, Massachusetts, USA) according to ISO 527-1993 and ISO 178-1993, respectively. The tensile test speed was 50 mm/min, and the sample length between bench marks was 50 ± 0.5 mm.

The notched Charpy impact strength of the samples was measured with a ZBC-4A impact testing machine from Xinsansi Co. (Shenzhen, China) according to ISO 180.

Reduced Viscosity

Samples of PA6 of about 0.5 g were dissolved in 100 mL of formic acid (88 wt %). The time of outflow of the solution was measured in an Ubbelohde viscometer (Kelong Co., Chengdu, China) in a water bath at 25°C according to ISO 307-1984. Then, the reduced viscosity was calculated with the following formula:

$$\eta = \left(\frac{t}{t_0} - 1\right) \times \frac{1}{C} \quad (1)$$

where t is the time of outflow of the PA6 solution (s), t_0 is the time of outflow of the solvent (s), and C is the concentration of the PA6 solution (g/mL).

End-Group Analysis.[17]

Carboxylic acid groups. Samples of PA6 of about 0.3 g were dissolved in 20 mL of phenylcarbinol at 150°C. Propyl alcohol (3 mL) was added, and the hot solution was titrated with NaOH (ca. 0.02 mol/L), with phenolphthalein as the indicator. The content of carboxylic acid (X) was calculated with the following formula:

$$X = \frac{(a-b)n}{W} \times 10^{-3} \quad (2)$$

where a is the volume of NaOH solution used by sample (mL), b is the volume of NaOH solution used by the solvent (mL), n is the molar concentration of the NaOH solution (mol/L), and W is the weight of the sample (g).

Terminal amine groups. Samples of PA6 of about 0.3 g were dissolved in 25 mL of a mixed solution of phenol and methyl alcohol (volume ratio = 1 : 1) at 55°C. The solution was titrated with HCl (ca. 0.005 mol/L) with thymol blue as the indicator. The content of terminal amine groups (Y) was calculated with the following formula:

$$Y = \frac{(A-B)^n}{W} \times 10^{-3} \quad (3)$$

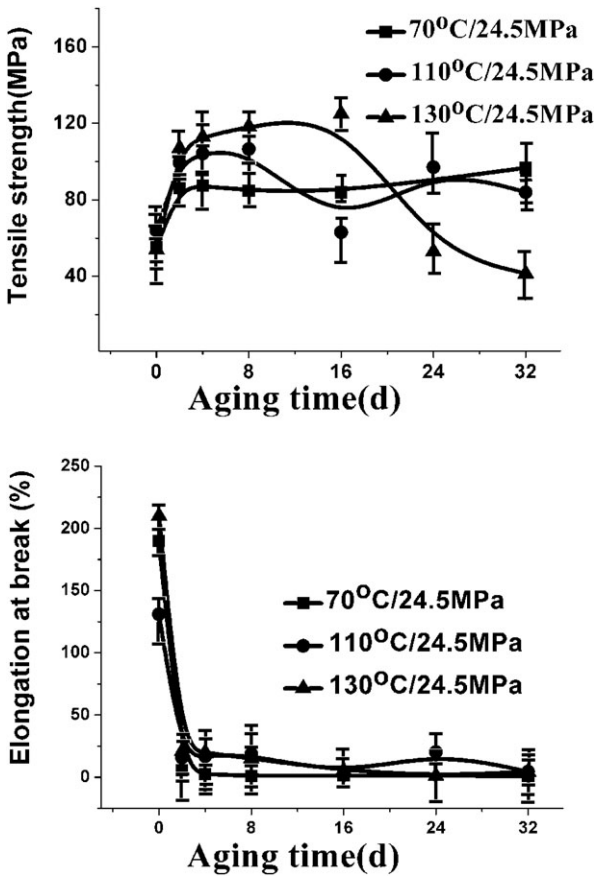

Figure 2. Mechanical properties of PA6 as a function of the aging time at different temperatures under 24.5 MPa.

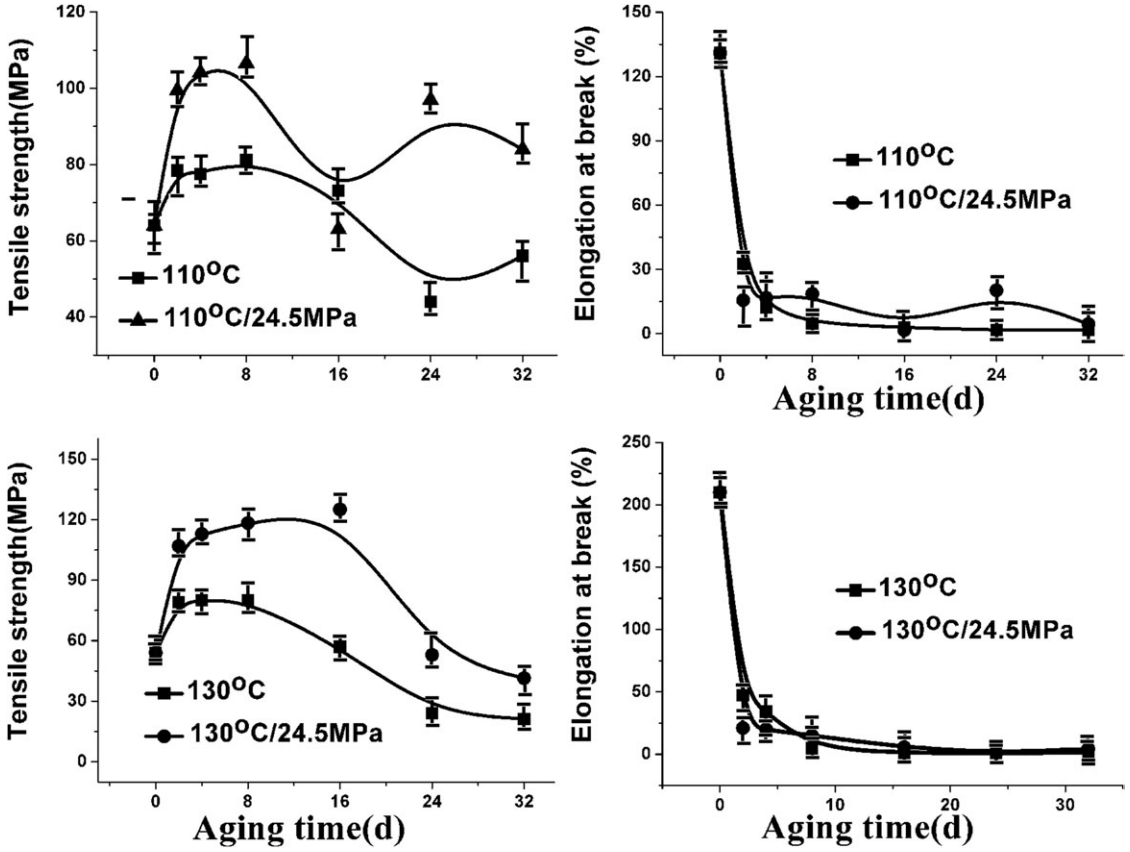

Figure 3. Mechanical properties of PA6 as a function of the aging time at high temperatures.

where A is the volume of HCl solution used by the sample (mL), B is the volume of HCl solution used by the solvent (mL), n is the molar concentration of the HCl solution (mol/L), and W is the weight of the sample (g).

UV Spectrum Analysis. Samples of PA6 of about 0.2 g were dissolved in 50 mL of a mixed solution of sulfuric acid and methanol (0.4 mol/L). The UV absorption measurements for the solutions for characterizing the structure during aging were carried out with a U3010 spectrophotometer (Hitachi Ltd., Tokyo, Japan).

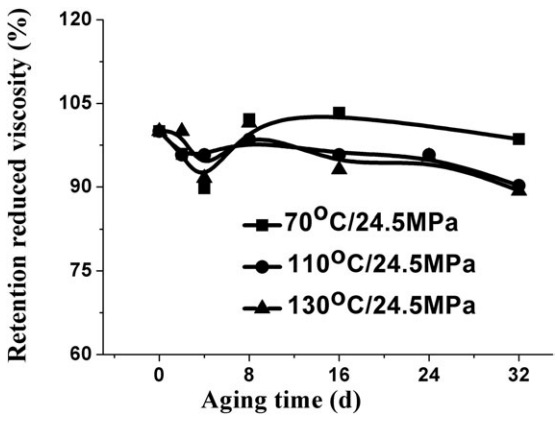

Figure 4. Reduced viscosity of PA6 as a function of the aging time at different temperatures under 24.5 MPa.

Nonisothermal Crystallization Analysis. Nonisothermal crystallization was performed with a Netzsch 204 Phoenix differential scanning calorimeter (Bavarian, Germany). The temperature scale of differential scanning calorimetry (DSC) was calibrated with indium. Granulated samples of about 10 mg were heated from ambient temperature to 250°C at a heating rate of 10°C/min under a nitrogen atmosphere. The quantity of heat absorbed during the melting of the polymer was substantively equivalent to that required to break down the crystal structure. The higher the crystallinity (X_c) was, the higher the melting heat was. X_c was calculated with the following formula:

$$X_c = \left(\frac{\Delta H_m}{\Delta H_0}\right) \times 100\% \quad (4)$$

where ΔH_m is the melting enthalpy and ΔH_0 is the balance melting enthalpy, that is, the melting enthalpy of 100% crystallizing PA6, which was 190 J/g.

Wide-Angle X-Ray Diffraction (WAXD) Analysis. WAXD analysis of PA6 at the start and end of aging was conducted with Bruker D8 diffractometer (Kanagawa, Japan) with Cu Kα radiation generated at 40 kV and 30 mA.

RESULTS AND DISCUSSION

Creep Behavior of PA6 during Thermooxidative Aging under Stress

The creep behaviors of PA6 subjected to a stress of 24.5 MPa at different temperatures were investigated. Figure 1 shows the

Applied Polymer SCIENCE

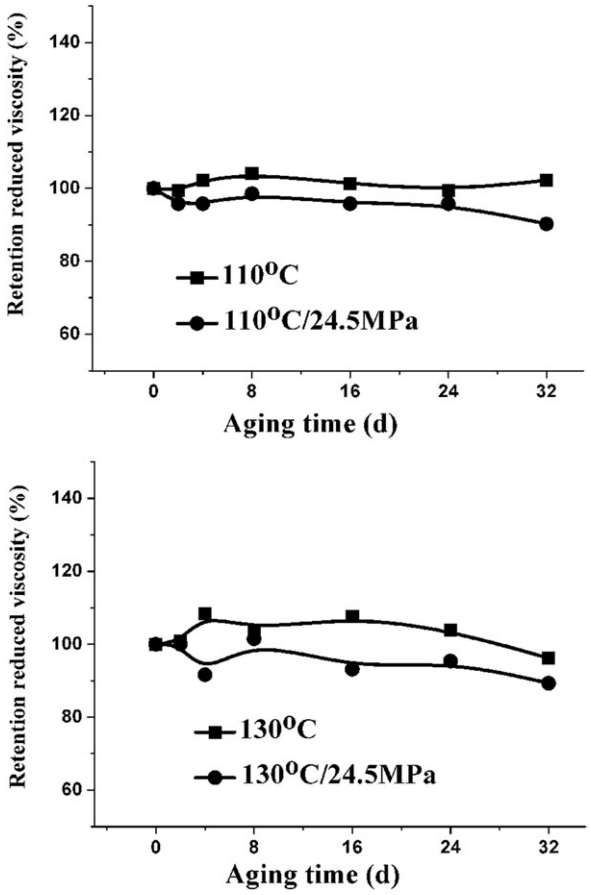

Figure 5. Retention of the reduced viscosity of PA6 as a function of the aging time at high temperatures.

variation of the creep deformation of PA6 with aging time. A similar change tendency in the creep deformation of all of the samples was observed. In the initial stage of aging, the creep deformation of the samples increased rapidly, and then after about 200–300 min, a platform was observed, and the creep deformation tended to be stable. X_c of PA6 was about 30%, and there existed a lot of amorphous area and free volume for molecular chains to move at the beginning of aging. This resulted in a remarkable increase of the creep deformation of PA6 under stress. With increasing aging time, the molecular chain arrangement became orderly under stress, the free volume decreased, and the movement of the molecular chain became slow and difficult. This resulted in a decrease in the creep rate.

Moreover, the creep deformation of PA6 became much higher and tended to increase more rapidly with aging temperature; this may have been due to an increase in the molecular mobility at high temperature.

Mechanical Properties of PA6 during Thermooxidative Aging under Stress

The mechanical properties of PA6 at different aging temperature and subjected to a constant stress are shown in Figure 2. The tensile strength of PA6 continued to increase with aging time and temperature during the first 8 days. Afterward, the subsequent variation of strength differed for PA6 aging at different temperatures. For PA 6 aged at 70°C, the tensile strength remained almost constant after 8 days of aging; however, when the temperature was increased to 110 or 130°C, the tensile strength was found to decrease afterward. The elongation at break of PA6 aging at different temperatures all decreased rapidly to a plateau with increasing aging time.

The mechanical properties of PA6 aged at high temperature (110 and 130°C) with and without stress were also investigated. As shown in Figure 3, the tensile strength of all of the PA6 samples increased at first and decreased afterward. However, the tensile strength of PA6 aged with stress was much higher than that of the sample aged without stress for the same aging time. The elongation at break values of all of the samples decreased sharply to the minimum.

The mechanical properties of PA6 aged only under thermal stress and oxygen could be induced by the so-called thermal embrittlement and oxidative embrittlement mechanisms. When the aging temperature was in the range of the glass transition temperature (T_g) to the peak melting temperature (T_m), there was an annealing process of PA6 at first. In this case, the internal stress of PA6

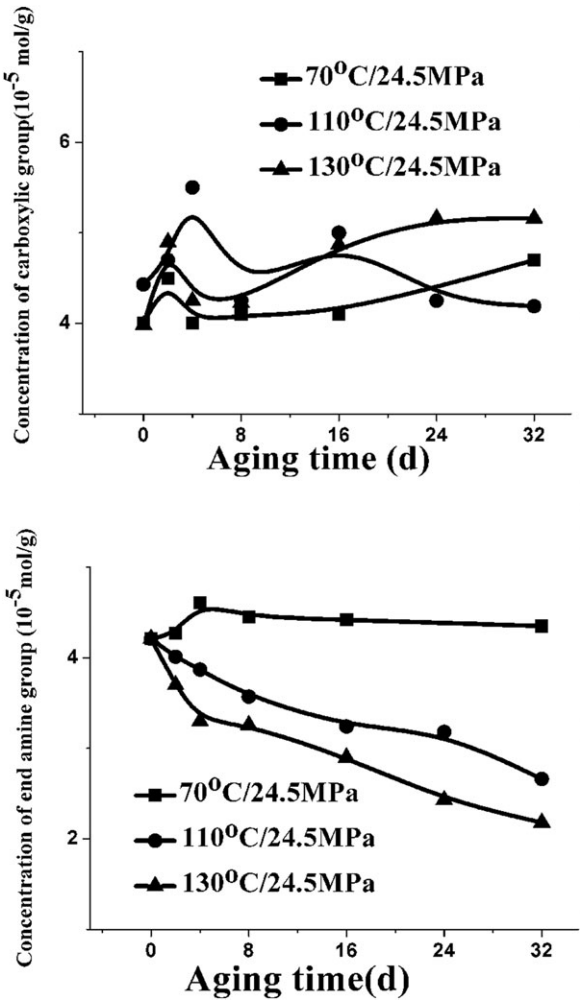

Figure 6. Concentrations of the end carboxylic groups and end amine groups of PA6 as a function of the aging time at different temperatures under 24.5 MPa.

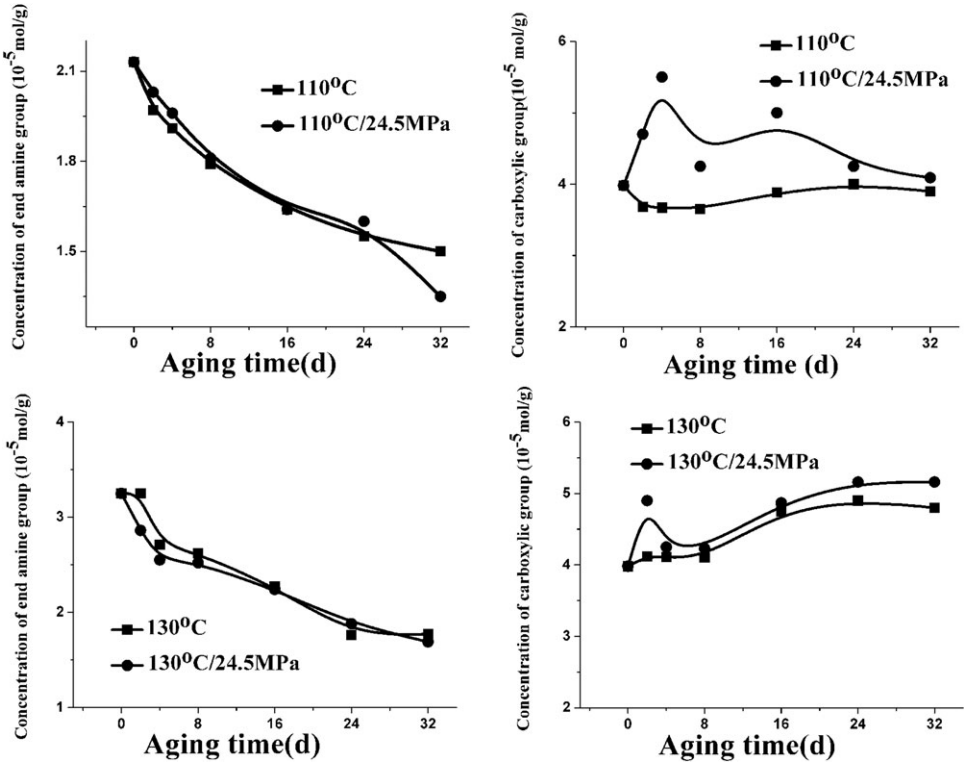

Figure 7. Concentrations of the end carboxylic groups and end amine groups of PA6 as a function of the aging time at high temperatures.

was reduced; meanwhile, the spherulites of PA6 grew bigger, and X_c increased. Therefore, in the primary stage of the aging process, the tensile strength and brittleness increased. At the same time, the crosslinking reaction dominated at this stage; this also made the tensile strength increase to some extent. However, with increasing aging time, molecular degradation dominated, and the remarkable decline of the molecular weight made the mechanical strength decrease greatly. During the whole oxidation process, the molecular weight distribution was widened, the regularity of the molecular chain became poor, and the hydrogen bonding and van der Waals forces between the molecules became weak. Also, the defects in the matrix increased, which resulted in a decline in the elongation at break of PA6.

For PA6 aging under stress, in addition to the thermal embrittlement and oxidative embrittlement mechanisms, the tensile strength substantially increased in the primary aging stage because of stress-induced crystallization and orientation. Moreover, the tensile strength increased rapidly with temperature. The higher the aging temperature was, the bigger the molecular mobility of PA 6 was. However, in the middle and last stages of aging, molecular degradation induced by stress and thermooxidation occurred, and the mechanical properties began to decline.

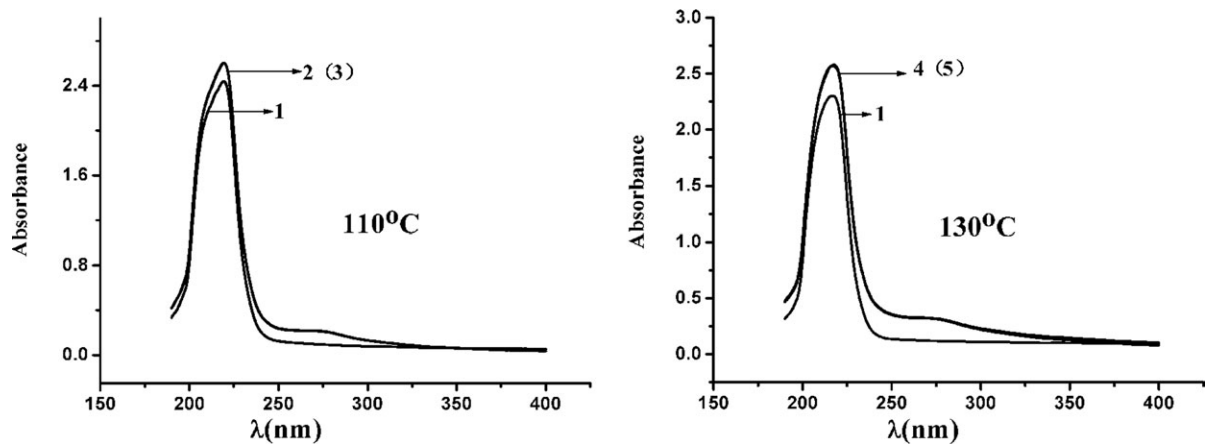

Figure 8. UV spectrum of PA6 at different aging temperatures under 24.5 MPa (in 0.4 mol/L sulfuric acid/methanol): (1) 0 day, (2) 110°C for 32 days, (3) 110°C at 24.5 MPa for 32 days, (4) 130°C and 32 days, and (5) 130°C at 24.5 MPa for 32 days.

Applied Polymer SCIENCE

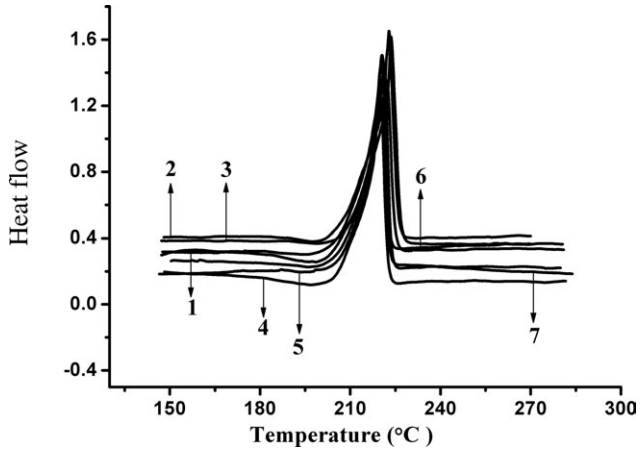

Figure 9. DSC curves of PA6 with a heating rate of 10 K/min: (1) PA6/0 days, (2) PA6 at 70°C for 32 days, (3) PA6 at 70°C and 24.5 MPa for 32 days, (4) PA6 at 110°C for 32 days, (5) PA6 at 110°C at 24.5 MPa and 32 days, (6) PA6 at 130°C for 32 days, and (7) PA6 at 130°C and 24.5 MPa for 32 days).

Table I. Melting Parameters of PA6 at Different Aging Temperatures under 24.5 MPa of Stress

No.	Sample	T_{onset} (°C)	T_{end} (°C)	T_m (°C)	X_c (%)
1	0 days	211.4	222.1	220.1	26.09
2	70°C/32 days	209.5	216.6	216.0	22.63
3	70°C/24.5 MPa/32 days	206.3	221.7	219.2	26.25
4	110°C/32 days	215.0	222.5	220.1	24.25
5	110°C/24.5 MPa/32 days	214.3	223.5	221.5	28.51
6	130°C/32 days	214.9	222.7	220.7	26.91
7	130°C/24.5 MPa/32 days	216.0	222.6	220.9	28.94

Reduced Viscosity of PA6 during Thermooxidative Aging under Stress

Throughout aging, changes in the reduced viscosity of PA6 were detected as a result of stress–thermooxidative degradation. As shown in Figure 4, the reduced viscosity of PA6 subjected to a stress of 24.5 MPa was plotted as a function of aging time at three aging temperatures, 70, 110, and 150°C. The reduced viscosity of PA 6 declined sharply at first and then reached a stable value. Furthermore, the reduced viscosity of the samples decreased at elevated temperatures. It is well known that the reduced viscosity characterizes the viscosity-average molecular weight of polymers.[18] Therefore, the results show that the molecular degradation led by the high temperature of PA6 predominated; this resulted in a decrease in the reduced viscosity.

A comparison of the reduced viscosity of PA6 aged under stress and without stress is shown in Figure 5. The samples of PA6 aged under stress had lower reduced viscosity values than the sample aged without stress; this indicated that the stress may have promoted the chain scission of PA6 during thermal aging.

Chemical Structure of PA6 during Thermooxidative Aging under Stress

The amido bond is considered to be the weakest bond in the molecule of PA. The rupture of the amido bond and the adjacent C—C bond resulted in the formation of the carboxylic acid, carbonyl, and end amine groups. The decline of the concentration of the end amine group of PA6 perhaps resulted from the reaction between end amine groups and carboxylic

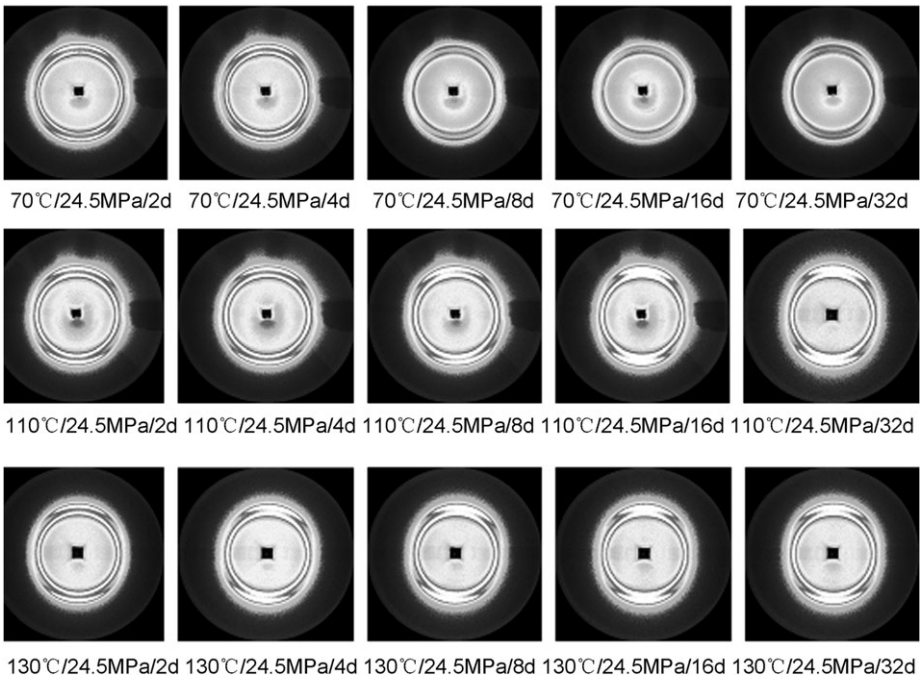

Figure 10. Two-dimensional XRD patterns of PA6 at different aging temperatures under 24.5 MPa.

Table II. *f* Values of PA6 at Different Aging Temperatures under 24.5 MPa

Time (days)	*f*		
	70°C/24.5 MPa	110°C/24.5 MPa	130°C/24.5 MPa
0	0.1397	0.1397	0.1397
2	0.2164	0.2927	0.3058
4	0.2820	0.3088	0.3186
8	0.2348	0.3273	0.3335
16	0.3732	0.3722	0.3830
24	/	0.3513	0.3585
32	0.4021	0.3651	0.3790

acids or the production of compounds such as tertiary amine or compounds escaped from the matrix by aging degradation. During the thermooxidative aging of PA6, the higher the concentration of the carboxylic acid was, the more quick the oxidation aging of the sample was, and the further the degradation of the polymers could be promoted. However, the end amine group had a thermal stabilization effect on PA. The variation of the chemical structure (the carboxylic acid and the amine end group) of PA6 with aging time at different temperatures is shown in Figure 6. With increasing aging time, the carboxylic acid concentration rose, and the end amine group concentration dropped monotonically for PA6. The carboxylic acid concentration of PA6 aged at a lower temperature was lower than that of the sample aged at a higher temperature, and its end amine group concentration was relatively higher during the whole aging process.

As shown in Figure 7, compared with samples aged only under heat and oxygen, the carboxylic acid concentration was higher for the sample aged under stress, whereas the difference in end amine group concentrations was not so remarkable.

UV spectra of various aged samples of PA6 are shown in Figure 8. The UV absorption of PA6 at bands of 220 and 250–290 nm increased after aging, whereas the variation tendency of the UV absorption of PA6 aging with and without stress was similar; this indicated that at the high temperature, the thermooxidation showed a larger effect on the structure of PA6 than the stress did.

After aging, the degradation products, including unsaturated aldehydes, ketones, carboxylic acids, and other compounds, were generated, and the $\pi \rightarrow \pi^*$ or $n \rightarrow \pi^*$ electron transition of carbonyl groups in these compounds may have resulted in an increase in the UV absorption at about 205 nm. However, the auxochrome group in the vicinity of carbonyl groups led to an n–π conjugation effect and resulted in a redshift of the corresponding UV absorption to 220 nm. The UV absorption at 260–290 nm was enhanced because of the formation of isolated carbonyl groups during aging. A series of degradation reactions were initiated, as shown next:

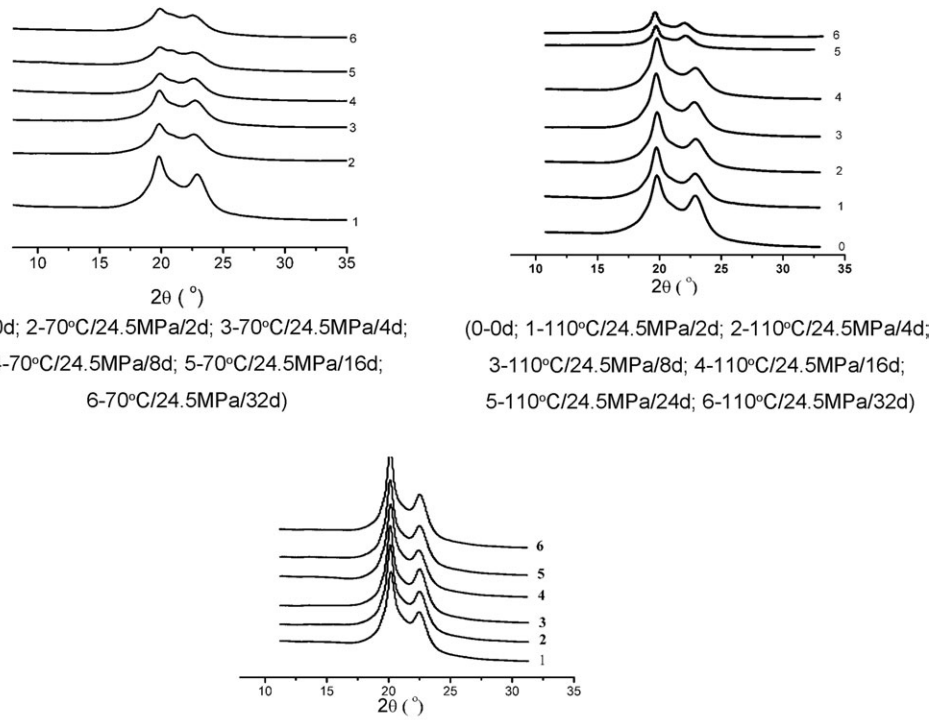

Figure 11. XRD curves of PA6 at different aging temperatures under 24.5 MPa.

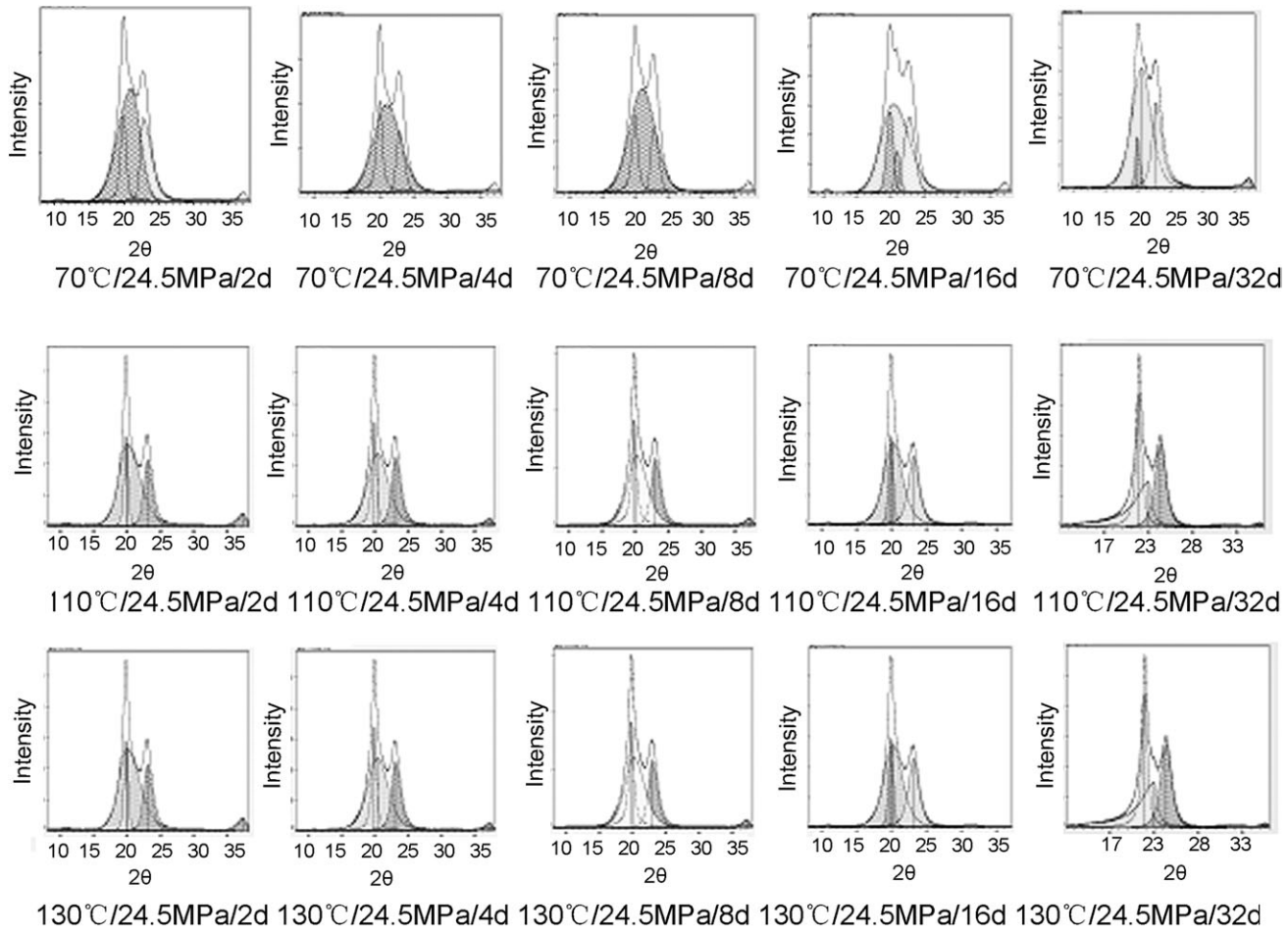

Figure 12. Deconvolution of WAXD curves of PA6 at different aging temperatures under 24.5 MPa.

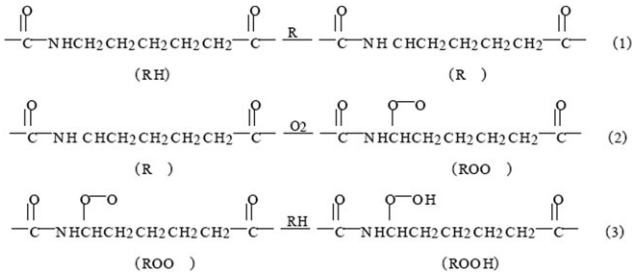

Crystallization and Orientation Behavior of PA6 during Thermooxidative Aging under Stress

The nonisothermal DSC curves of various aged samples of PA6 with a heating rate of 10 K/min are shown in Figure 9; from these, the onset melting temperature (T_{onset}), the end melting temperature (T_{end}), T_m, and X_c could be obtained, as listed in Table I. It can be seen that the measurement of the crystalline fraction showed an increase in X_c for the stress-aged sample; this indicated the fact that stress could induce the crystallization of PA.

The temperatures at which PA6 reached the maximum rates of crystallization (T_{max}'s) were calculated with the following empirical formula:

$$T_{max} = 0.63T_m + 0.37T_g - 18.5 \quad (5)$$

where T_m is the peak melting temperature of PA6 and T_g is the glass-transition temperature of PA6.

The calculated T_{max} was about 130°C for PA6; therefore, X_c of PA6 aged under this temperature remained at a relatively high level.

The WAXD patterns of various aged samples of PA6 are shown in Figure 10. When PA 6 was subjected to stress and with increasing aging time, its (200) reflection became narrower in spread and more prominent; this suggested that the crystal axis was oriented. Moreover, the degree of orientation tended to increase at high aging temperatures; this may have been due to an increase in the molecular mobility.

According to Herman's orientation model, as shown in eqs. (6)–(8), the orientation factor (f) of PA6 could be calculated, and the data are listed in Table II:

$$f = \frac{3 < \cos^2 \phi > -1}{2} \quad (6)$$

$$\cos^2 \phi = \frac{\int_0^{\frac{\pi}{2}} I(\phi) \sin\phi (\cos^2 \phi) d\phi}{\int_0^{\frac{\pi}{2}} I(\phi) \sin\phi d\phi} \quad (7)$$

Table III. X_c Values of PA6 at Different Aging Temperatures under 24.5 MPa of Stress

	X_c (%)		
Time (days)	70°C/24.5 MPa	110°C/24.5 MPa	130°C/24.5 MPa
0	30.12	30.12	30.12
2	34.18	34.29	34.56
4	34.49	34.43	34.96
8	35	36.58	36.68
16	36.2	37.15	37.90
24	—	35.23	35.94
32	37	36.01	36.48

$$\cos\phi = \cos\theta \times \cos u \tag{8}$$

where θ is the Bragg diffraction angle and u is the angle between the normal of the crystal surface and the tensile direction. ϕ is the angle between the chain axis and a reference axis z; I is the intensity of photons.

A one-dimensional X-ray diffraction curve corresponding to the two-dimensional diffraction pattern is shown in Figure 11. The intensity of the diffraction peak represented the degree of the order in the material, including crystallization and orientation. It can be seen that the diffraction peak position of aged PA6 showed no change, however, there were significant differences in intensity, and this indicated that stress aging did not affect the crystal type, but it could significantly affect the crystallization and orientation of PA6.

Figure 12 shows the corresponding decomposed WAXD curves obtained by PeakFit software (SeaSolve Software Inc., Framingham, Massachusetts, USA), and X_c of PA6 was calculated from the peak area of the crystalline and amorphous regions, as summarized in Table III.

As shown in Table II, X_c and f of PA6 increased with aging temperature; this indicated the formation of a clear orientation and the crystallization of molecules induced by stress. However, X_c and f decreased after 16 days; this demonstrated that stress-induced degradation occurred, and the molecular orientation was weakened. Moreover, with increasing aging temperature, both X_c and f of PA6 exhibited an increasing tendency, which resulted from the increasing mobility of the molecular chain at high temperatures.

CONCLUSIONS

The long-term stress-accelerating aging behavior of PA6 was studied at relatively high temperatures (70, 110, and 130°C). The results show that a remarkable increase in the creep deformation of PA6 under stress was observed at the beginning of aging, and the creep deformation of PA6 was much higher and tended to increase more rapidly with increasing aging temperature. The tensile strength of PA6 subjected to a constant stress increased with aging time and temperature during the first 8 days. Afterward, it was found to decrease at elevated temperatures. The tensile strength of PA6 aged with stress was much higher than that of the sample aged without stress. The reduced viscosity of PA 6, which decreased at elevated temperatures, declined sharply at first and then reached a stable value because of the molecular degradation under heat. The samples aged under stress had a lower reduced viscosity than that of the sample aged without stress; this indicated that the stress may have promoted the chain scission of PA6 during thermal aging. With increasing aging time, the carboxylic acid concentration rose, and the end amine group concentration dropped monotonically for PA6. Compared with samples aged without stress, the carboxylic acid concentration was higher for the sample aged under stress. The UV absorption of PA6 at bands of 220 and 250–290 nm increased after aging, whereas the whole variation tendency of the UV absorption of PA6 aged with and without stress was similar. f and X_c of PA6 increased during the first 16 days; this indicated of a clear orientation and crystallization of molecules induced by stress. Then, X_c and f decreased; this demonstrated that stress-induced degradation occurred, and the molecular orientation was weakened. Moreover, with increasing aging temperature, both X_c and f of PA6 exhibited an increasing tendency; this resulted from the increasing mobility of the molecular chain at high temperatures.

ACKNOWLEDGMENT

This work was supported by the Key Natural Science Fund of China (contract grant number 51133005).

REFERENCES

1. Sangkeun Rhee, J. L. *White, Polymer* **2002**, *43*, 5903.
2. Hagler, A. T.; Lapiccirella, A. *Biopolymers* **1976**, *15*, 1167.
3. Sargar, B. F. *J. Chem. Soc.* **1967**, *B248*, 1047.
4. Šebenda, J.; Lánská, B. *J. Macromol. Sci. Chem.* **1993**, *30*, 669.
5. Lánská, B. *Eur. Polym. J.* **1994**, *30*, 197.
6. Gröning, M.; Hakkarainen, M. *J. Chromatogr. A* **2001**, *932*, 1.
7. Du, Y.; Gong, J. X. *Adhes. Chin.* **2005**, *26*, 41.
8. Lehrle, R. S.; Parsons, I. W.; Rollinson, M. *Polym. Degrad. Stab.* **2000**, *67*, 21.
9. Jain, A.; Vijayan, K. *J. Mater. Sci.* **2002**, *37*, 2623.
10. Pramoda, K. P.; Liu, T, Liu, Z.; He, C. B.; Sue, H. *J. Polym. Degrad. Stab.* **2003**, *81*, 47.
11. Cerruti, P.; Carfagna, C.; Rychly, J.; Matisová-Rychlá, L. *Polym. Degrad. Stab.* **2003**, *82*, 477.
12. Cerruti, P.; Carfagna, C. *Polym. Degrad. Stab.* **2010**, *95*, 2405.
13. Shu, Y.; Ye, L.; Yang, T. *J. Appl. Polym. Sci.* **2008**, *110*, 945.
14. Dan, E.; Demco, V.; Litvinov, M.; Rata, G. *Macromol. Chem. Phys.* **2007**, *208*, 2085.
15. Kiliaris, P.; Papaspyrides, C. D, Pfaendner, R. *Polym. Degrad. Stab.* **2009**, *94*, 389.
16. Jacobson, K.; Stenberg, B.; Terselius, B. *Polym. Degrad. Stab.* **1999**, *65*, 449.
17. Skrypnyk, I. D.; Hoekstrab, H. D.; Spoormake, J. L. *Polym. Degrad. Stab.* **1998**, *60*, 21.
18. He, M. Polymer Physics; Fudan Industry: Shanghai, China, **2002**.